J. Membrane Biol. 85, 121–132 (1985)

The Journal of
Membrane Biology

Compartment Analysis of Plant Cells by Means of Turgor Pressure Relaxation: I. Theoretical Considerations

Stephan Wendler† and Ulrich Zimmermann‡

†Arbeitsgruppe Membranforschung am Institut für Medizin der Kernforschungsanlage Jülich, 5170 Jülich, Federal Republic of Germany and ‡Lehrstuhl für Biotechnologie der Universität Würzburg, 8700 Würzburg, Federal Republic of Germany

Summary. Turgor pressure relaxation curves for individual plant cells represent an important source of information for the plant physiologist. However, the accurate interpretation of these curves is strongly dependent on the model chosen to describe the plant cell. If the compartmentation of the cell into vacuole and cytoplasm is taken into account, a theoretical analysis shows that pressure relaxation curves can be represented by the sum of two exponential functions. Given *a priori* assumptions about the exchange area of the tonoplast and its reflection coefficient, the hydraulic conductivities of the plasmalemma and tonoplast can be determined and the proportion of the total cell volume occupied by the cytoplasm is also obtained. Numerical solutions to the flow equations have shown that the biphasic nature of pressure relaxations is maintained even when a permeable tonoplast is assumed. Depending on the magnitude of the reflection coefficient and the permeability of the vacuolar membrane, large errors can arise in the determination of the hydraulic conductivity of the tonoplast. However, under certain conditions, even a highly permeable tonoplast may behave like a nonpermeable membrane during pressure relaxation.

Key Words compartment analysis · turgor pressure · relaxation · tonoplast · plasmalemma · hydraulic conductivity · cytoplasmic volume

Introduction

In many plant cells the vacuole occupies most of the cell interior, and the cytoplasm is reduced to a thin layer between the plasmalemma and the vacuolar membrane, the tonoplast. For this reason, the cellular hydraulic conductivity (L_p) deduced from transcellular osmosis [4, 5], pressure probe [18] and labeled flux measurements [17] is a characteristic of the total membrane barrier system consisting of the tonoplast, cytoplasm, plasmalemma and cell wall [3]. Attempts have been made to differentiate the hydraulic properties of the tonoplast and plasmalemma by removing one of the membranes by chemical destruction and measuring the hydraulic conductivity of the remaining membrane alone [7, 14]. Url [14] investigated the primary site of resistance to the penetration of water in the protoplasm of inner epidermal cells of the *Allium cepa* bulb scale. After repeated deplasmolysis, some surviving cells formed a tonoplast. The hydraulic conductivity of the tonoplast was calculated from the swelling characteristics of this membrane. Kiyosawa and Tazawa [7] followed another approach to the problem. They claimed to have removed the tonoplast of *Chara* cells using a perfusion medium containing EGTA. However, pressure probe measurements (Wendler, Zimmermann and Shimmen, *unpublished results*) and charge pulse experiments (Benz and Zimmermann, *unpublished results*) showed that the plasmalemma was damaged by this chemical treatment, and there were indications that not every perfusion resulted in complete removal of the tonoplast. As the chemical removal of the tonoplast has been inferred from indirect observations only, an alternative method for the determination of the hydraulic conductivities of both the plasmalemma and the tonoplast is desired.

In this and the accompanying paper, a method of measuring the hydraulic conductivities of the plasmalemma and the tonoplast which does not disturb the integrity of the cells will be presented. The method utilizes the wealth of information obtained from pressure relaxation curves when analyzed using a modified high-resolution technique. This paper deals with a theoretical analysis of pressure relaxations in the light of an expanded model of the cell, while the second paper (henceforth referred to as paper II) will deal with the experimental confirmation of the theoretical predictions relating to the fresh-water alga *Chara corallina*.

Principles

A relaxation describes the behavior of a system as it moves towards a new state of equilibrium after a

sudden shift away from equilibrium. If the system is a plant cell and the equilibrium is disturbed by a shift in osmotic or hydrostatic pressure, the cell achieves a new equilibrium by way of a pressure relaxation. Using the pressure probe technique, it is possible to monitor both hydrostatically and osmotically induced turgor pressure relaxations in plant cells.

The time course of a pressure relaxation is determined by the elastic properties of the cell wall (ε) and the hydraulic conductivity of the total membrane barrier system (Lp) [2, 20–22]. The volumetric elastic modulus can be measured independently while pressure relaxations are normally used to determine Lp. The interpretation of the relaxation curves, however, depends both on the resolution of the pressure-measuring device and on the model used to describe a plant cell.

The conventional model of a plant cell used when analyzing pressure relaxation curves is a two-compartment model. It assumes that the external space and cell interior are separated by a single barrier. The Lp data reported in the literature [1, 3, 10, 11, 18, 19, 21] are based on this model. However, the plasmalemma and the tonoplast should not be equated this way because the mathematical description of the system then provides for a pressure gradient across the entire membrane barrier system. This is in contrast to the real situation, since a hydrostatic pressure gradient (i.e. turgor pressure) is possible only across the cell-wall/plasmalemma barrier and not across the tonoplast. The simple view of the two-compartment model is only justified when the properties of tonoplast and cytoplasm can be neglected.

Published work indicates that the hydraulic conductivity of the cytoplasm is large compared to that of plant cell membranes [12, 14]. However, the hydraulic conductivity of the tonoplast can be neglected only if it is much larger than that of the plasmalemma.

A more complete model, referred to here as the three-compartment model, takes into account the internal compartmentation of the cell into vacuole and cytoplasm by the tonoplast. The three-compartment model is described in detail, starting with an analytical solution of the water flow equations. In the context of this model, a single turgor pressure relaxation in an intact cell is shown to yield information on the Lp values of the plasmalemma and the tonoplast. The contribution of the cytoplasmic volume to cell volume can be estimated from the same curve without additional measurements.

Next the numerical solution to the flow equations is used to examine the influence of solute flow at the tonoplast on turgor pressure relaxations.

The Three-Compartment Model

Tyree [13] showed by *numerical* solution of the flow equations that the change in cell turgor with time, following a disturbance from the equilibrium state, does not exhibit a simple exponential course if the water conductivity of the tonoplast and the internal compartmentation of the cell into vacuole and cytoplasm are considered. In the following, we will demonstrate that the phenomenological equations for water flow at the plasmalemma and tonoplast can be solved *analytically* and that the change of turgor with time, following a disturbance, is represented by the superposition of two exponential functions. We assume that solute flow J_s at both membranes can be neglected. The following analysis, therefore, is valid when the external medium contains only impermeable or weakly permeable substances (reflection coefficient $\sigma \simeq 1$, solute permeability $\omega \simeq 0$). The effect of possible solute flows at the tonoplast will be examined in the next chapter. The calculations are based on the model shown in Fig. 1. The three nested compartments represent the external space (1), the cytoplasm (2) and the vacuole (3), respectively, and are separated by the membranes p and t (plasmalemma and tonoplast). Both hydrostatic and osmotic pressure gradients can be established across membrane p, while membrane t is subject only to an osmotic pressure gradient. The solutions in compartments 1, 2 and 3 contain impermeable and weakly permeable solutes. The solutions are well stirred in all areas so that the concentration in the individual compartments is homogeneous at all times. The outside compartment is large compared to the cell volume so that the osmotic pressure of the bathing solution can be considered as constant. It is assumed that the concentration differences across the membranes are small compared with the concentrations in the cell compartments. The volume flows through the plasmalemma and the tonoplast are equal to the water flow when solute flow is neglected. Adapting the convention of positive flow being from outside to inside and defining the pressure of the external compartment as zero, the water flow is described by the following equations derived from the thermodynamics of irreversible processes [6, 10]:

$$J_{vp} = Lp_p\{P - (\pi_2^i - \pi_1^i) - \sigma_p(\pi_2^s - \pi_1^s)\} \quad (1)$$

$$J_{vt} = -Lp_t\{(\pi_3^i - \pi_2^i) + \sigma_t(\pi_3^s - \pi_2^s)\} \quad (2)$$

where J_{vp} = volume flow across the plasmalemma, J_{vt} = volume flow across the tonoplast, Lp_p = hydraulic conductivity of the plasmalemma, Lp_t = hydraulic conductivity of the tonoplast, σ_p = reflec-

tion coefficient of the plasmalemma for permeable solute, σ_t = reflection coefficient of the tonoplast for permeable solute, P = turgor pressure, π = osmotic pressure, i = impermeable solute (superscript), s = permeable solute (superscript) and 1,2,3 = compartments 1, 2 and 3 (subscript).

For $t < 0$ the cell is assumed to be in equilibrium with the external space. For $J_{vp} = 0$ and $J_{vt} = 0$, the following relationship is obtained for the equilibrium turgor P_o and the osmotic pressures of the inner compartments π^r_{ko} ($k = 2,3$; $r = i,s$):

$$P_o = (\pi^i_{2o} - \pi^i_1) + \sigma_p(\pi^s_{2o} - \pi^s_1)$$
$$= (\pi^i_{2o} + \sigma_p \cdot \pi^s_{2o}) - (\pi^i_1 + \sigma_p \cdot \pi^s_1) \quad (3)$$
$$\pi^i_{2o} + \sigma_t \cdot \pi^s_{2o} = \pi^i_{3o} + \sigma_t \cdot \pi^s_{3o}. \quad (4)$$

Equation (3) implies that turgor pressure is balanced by an osmotic pressure gradient, and Eq. (4) emphasizes that the turgor pressures in compartments 2 and 3 are equal at equilibrium.

For the sake of brevity, the following symbols are introduced for the effective osmotic pressures:

$$\pi^*_1 := \pi^i_1 + \sigma_p \cdot \pi^s_1 \quad (5)$$
$$\pi^*_{op} := \pi^i_{2o} + \sigma_p \cdot \pi^s_{2o} \quad (6)$$
$$\pi^*_{ot} := \pi^i_{2o} + \sigma_t \cdot \pi^s_{2o} = \pi^i_{3o} + \sigma_t \cdot \pi^s_{3o}. \quad (7)$$

It should be emphasized that these symbols must not be interpreted as osmotic pressures of a certain compartment. The indices p and t imply that these symbols are linked to a membrane rather than to a compartment. Equations (6) and (7) imply that π^*_{op} and π^*_{ot} are not equal if the reflection coefficients of the plasmalemma and the tonoplast are unequal. In terms of these abbreviations, Eq. (3) can be written as $P = \pi^*_{op} - \pi^*_1$.

In the following, a hydrostatically induced pressure relaxation is analyzed. At time $t = 0$, the system is moved from equilibrium by changing the turgor pressure from P_o to a value $P_i \neq P_o$. The permeability of the membranes to solutes is assumed to be low compared to the membrane permeability to water. Therefore, the contribution of solute flow to the change in the osmotic pressures in the cell compartments is negligible in comparison to that caused by water flow. For the tonoplast, even higher permeabilities can be permitted before it is necessary to take solute flow into account (*see* next chapter).

The change of the osmotic pressures in the cell compartments after the disturbance ($t > 0$) can be expressed by the volume changes of the relevant compartments. The following equations hold for the cytoplasm:

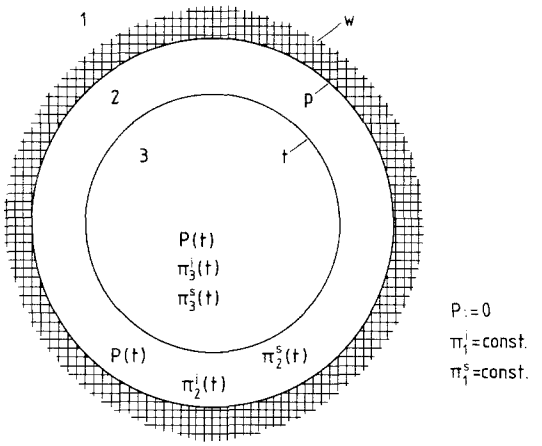

Fig. 1. Three-compartment model of the plant cell. The space is divided into external space (1) and the cell compartments cytoplasm (2) and vacuole (3). The nested compartments are separated by the plasmalemma (p) and the tonoplast (t). Across the membrane t, only an osmotic pressure gradient can be built up, whereas an additional hydrostatic pressure gradient (turgor pressure) is present across membrane p. Turgor pressure P develops due to the presence of an elastic cell wall (w). During a relaxation, the osmotic pressures (π^i_2, π^s_2, π^i_3, π^s_3) and the turgor pressure in the compartments 2 and 3 are functions of time. The hydrostatic pressure of the external space is zero by definition and the osmotic pressures of the solutes (π^i_1, π^s_1) are constant

$$\pi^r_2(t) = \pi^r_{2o} \cdot \frac{V_2}{V_2 + \Delta V_2(t)} \simeq \pi^r_{2o}\left[1 - \frac{\Delta V_2(t)}{V_2}\right]_{(r=i,s)} \quad (8)$$

and for the vacuole:

$$\pi^r_3(t) = \pi^r_{3o} \cdot \frac{V_3}{V_3 + \Delta V_3(t)} \simeq \pi^r_{3o}\left[1 - \frac{\Delta V_3(t)}{V_3}\right]_{(r=i,s)} \quad (9)$$

where V_2, V_3 are the compartment volumes at equilibrium ($t \leq 0$) and ΔV_2, ΔV_3 are the volume changes in each compartment ($t > 0$). The approximations at the right are valid for $\Delta V_2(t)/V_2 \ll 1$ and $\Delta V_3(t)/V_3 \ll 1$.

The net volume change of the cytoplasm during the pressure relaxation consists of the water flow between the external space and the cytoplasm and of the flow between the cytoplasm and the vacuole. Let $\Delta V'$ denote the volume change of the cytoplasm due to the water exchange with the outside compartment (positive for water influx and negative for water efflux), and let ΔV_3 denote the volume change of the vacuole (positive when vacuolar volume is increased and negative when it is decreased). Since a volume change of the vacuole can be effected only by a water exchange with the cytoplasm, the net volume change of the cytoplasm during the pressure relaxation ΔV_2 may be written as:

$$\Delta V_2(t) = \Delta V'(t) - \Delta V_3(t). \quad (10)$$

The amount of volume $\Delta V'$ exchanged with the outside is directly related with a pressure change ΔP by Eq. (11):

$$\Delta V'(t) = \frac{V_o}{\varepsilon} \cdot \Delta P(t) = \frac{V_o}{\varepsilon} (P(t) - P_i) \tag{11}$$

where ε is the volumetric elastic modulus of the cell wall, and V_o is the cell volume prior to the relaxation. Combining Eqs. (8), (10) and (11) the osmotic pressure of the substances (i,s) dissolved in the cytoplasm can be represented by:

$$\pi_2^r(t) = \pi_{2o}^r \left[1 - \frac{V_o}{V_2} \cdot \frac{\{P(t) - P_i\}}{\varepsilon} + \frac{\Delta V_3(t)}{V_2}\right]_{(r=i,s)}. \tag{12}$$

By substituting Eqs. (9) and (12) into Eqs. (1) and (2), rearranging, and ordering related terms, we obtain Eqs. (13) and (14) for the volume flows across the plasmalemma and the tonoplast:

$$J_{vp} = Lp_p \left[\left[1 + \frac{\pi_{op}^* \cdot V_o}{\varepsilon \cdot V_2}\right] \cdot P(t) - \frac{\pi_{op}^*}{V_2} \cdot \Delta V_3(t) - \pi_{op}^* \left[1 + \frac{P_i \cdot V_o}{\varepsilon \cdot V_2}\right] + \pi_1^*\right] \tag{13}$$

$$J_{vt} = -Lp_t \cdot \pi_{ot}^* \cdot \frac{V_o}{V_2} \left[\frac{1}{\varepsilon} \cdot P(t) - \frac{1}{V_3} \cdot \Delta V_3(t) - \frac{P_i}{\varepsilon}\right] \tag{14}$$

where $V_o = V_2 + V_3$ and the effective osmotic pressures (π_{op}^*, π_{ot}^*) were defined in Eqs. (6) and (7). The following equations also hold for J_{vp} and J_{vt}. The negative signs indicate that the positive direction of water flow is from inside to outside (i.e. $\Delta V' < 0$).

$$J_{vp} = -\frac{1}{A_p} \cdot \frac{d\Delta V'(t)}{dt} = -\frac{V_o}{A_p \cdot \varepsilon} \cdot \frac{dP(t)}{dt} \tag{15}$$

$$J_{vt} = -\frac{1}{A_t} \cdot \frac{dV_3(t)}{dt} = -\frac{1}{A_t} \cdot \frac{d\Delta V_3(t)}{dt} \tag{16}$$

where A_p = area of exchange of the plasmalemma and A_t = area of exchange of the tonoplast.

Combining Eq. (13) with Eq. (15) and Eq. (14) with Eq. (16), a system of two coupled linear differential equations results with the general form:

$$\dot{P} + a \cdot P + b \cdot \Delta V_3 = c; \quad \dot{P} := dP/dt \tag{17}$$

and

$$\Delta\dot{V}_3 + d \cdot \Delta V_3 + e \cdot P = f; \quad \Delta\dot{V}_3 := d\Delta V_3/dt \tag{18}$$

where the parameters a to f are given by:

$$a = A_p \cdot Lp_p \left[\frac{\varepsilon}{V_o} + \frac{\pi_{op}^*}{V_2}\right] \tag{19a}$$

$$b = -A_p \cdot Lp_p \cdot \pi_{op}^* \frac{\varepsilon}{V_o \cdot V_2} \tag{19b}$$

$$c = A_p \cdot Lp_p \frac{\varepsilon}{V_o} \left[\pi_{op}^* + \pi_{op}^* \cdot \frac{P_i}{\varepsilon} \cdot \frac{V_o}{V_2} - \pi_1^*\right] \tag{19c}$$

$$d = A_t \cdot Lp_t \cdot \pi_{ot}^* \frac{V_o}{V_2 \cdot V_3} \tag{19d}$$

$$e = -A_t \cdot Lp_t \cdot \pi_{ot}^* \frac{V_o}{\varepsilon \cdot V_2} \tag{19e}$$

$$f = -A_t \cdot Lp_t \cdot \pi_{ot}^* \frac{P_i \cdot V_o}{\varepsilon \cdot V_2}. \tag{19f}$$

These first-order differential equations can be transformed into a single second-order differential equation (Appendix A):

$$\ddot{P} + (a + d) \cdot \dot{P} + (a \cdot d - b \cdot e) \cdot P + (b \cdot f - d \cdot c) = 0 \tag{20}$$

with $\ddot{P} := d^2P/dt^2$.

The solution to this equation is the sum of (i) the solution to the homogeneous equation $\ddot{P} + (a + b) \cdot \dot{P} + (a \cdot d - b \cdot e) \cdot P = 0$ and (ii) a special solution to the inhomogeneous Eq. (20), for which a constant P_e can be taken [8]. Here we arrive at the central equation of the three-compartment model:

$$P(t) = \alpha_1 \cdot e^{k_1 \cdot t} + \alpha_2 \cdot e^{k_2 \cdot t} + P_e \tag{21}$$

where

$$k_{1,2} = -\frac{a + d}{2} \pm \sqrt{\frac{(a - d)^2}{4} + b \cdot e} \tag{22}$$

and

$$P_e = \frac{(d \cdot c - b \cdot f)}{(a \cdot d - b \cdot e)}. \tag{23}$$

Equation (21) shows that the time dependence of turgor pressure relaxation after a disturbance of the equilibrium condition by a change in turgor pressure can be described by the sum of two exponential functions. As has previously been well demonstrated for isotope flows among serial compartments [15], so also for volume flows under osmotic gradients, the two observable rate constants are complicated functions of all system parameters.

The appearance of two relaxation components can be explained in the following simplified way. When the cell turgor is increased by means of a volume change with the aid of the pressure probe, a

hydrostatic pressure gradient is established across the plasmalemma but not across the tonoplast. Initially, the net volume flow is determined only by the hydraulic conductivity of the plasmalemma. The volume loss, i.e. the water flow to the outside, brings about an increase in the osmotic pressure of the cytoplasm. Since the osmotic pressures of the cytoplasm and vacuole were equal initially, only now is an osmotic pressure gradient established across the tonoplast. This results in osmotically driven water flow from the vacuole into the cytoplasm. Therefore, a second conductivity, the hydraulic conductivity of the tonoplast, now influences the net flow to the outside compartment. If the hydraulic conductivity of the tonoplast is not substantially higher than that of the plasmalemma, the kinetics of water transport must slow down correspondingly. The same considerations apply—with reversed signs and reversed directions of flow—to a relaxation following a decrease in pressure.

If the resolution of a pressure relaxation is high enough, amplitudes and half-times of the two exponential components are experimentally accessible. The parameters α_1, α_2, k_1 and k_2 are clearly defined by the cell parameters. Therefore, four linear independent equations must exist which can be resolved into various cell parameters and thus be used for their calculation. Two such equations are given by Eqs. (24) and (25) and these follow from a combination of Eqs. (17), (21) and (23) with the boundary conditions $P(t = 0) = P_i$ and $\Delta V_3(t = 0) = 0$:

$$\alpha_1 \cdot k_1 + \alpha_2 \cdot k_2 + a \cdot P_i = c \tag{24}$$

$$\alpha_1 + \alpha_2 - \frac{(b \cdot f - d \cdot c)}{(a \cdot d - b \cdot e)} = P_i \tag{25}$$

or rearranged:

$$c - a \cdot P_i = \alpha_1 \cdot k_1 + \alpha_2 \cdot k_2 \tag{26}$$

$$\frac{(b \cdot f - d \cdot c)}{(a \cdot d - b \cdot e)} + P_i = \alpha_1 + \alpha_2. \tag{27}$$

Two further expressions are obtained by forming linear combinations of k_1 and k_2 from Eq. (22). The following system of equations is obtained:

$$(a - d)^2 + 4 \cdot b \cdot e = (k_1 - k_2)^2 \tag{28}$$

$$a + d = -(k_1 + k_2). \tag{29}$$

Equations (26) to (29) are suitable for the determination of the hydraulic conductivity of the plasmalemma (Lp_p) and the calculation of the effective osmotic pressure of the cytoplasm as controlled by the plasmalemma (π^*_{op}). Furthermore, the volume proportion occupied by the cytoplasm (V_2/V_o) and the product of the effective osmotic pressure of the vacuolar sap, the surface area and the hydraulic conductivity of the tonoplast ($\pi^*_{ot} \cdot A_t \cdot Lp_t$) can be calculated. Since the resolution of the equations into the corresponding cell parameters with the aid of Eqs. (19a) to (19f) and the equilibrium relation from Eq. (3) is troublesome but not difficult, the calculations are not presented here. The important results are:

$$Lp_p = \frac{V_o}{\varepsilon \cdot A_p} \cdot q \tag{30}$$

$$\pi^*_{op} = \varepsilon \cdot z \tag{31}$$

$$\frac{V_2}{V_o} = -\frac{q^2 \cdot z \cdot (1 + z)}{\{q^2 + (k_1 + k_2) \cdot q\} \cdot (1 + z) + k_1 \cdot k_2} \tag{32}$$

$$Lp_t \cdot A_t \cdot \pi^*_{ot} = -\frac{V_2 \cdot V_3}{V_o} \cdot \left\{k_1 + k_2 + q \cdot \left(1 + \frac{V_o}{V_2} \cdot z\right)\right\} \tag{33}$$

with $q := \dfrac{\alpha_1 \cdot k_1 + \alpha_2 \cdot k_2}{P_o - P_i}$ and $z := \dfrac{P_e - P_o}{P_i - P_e}$.

These equations must be discussed in more detail because they are the key equations for a compartment analysis of plant cells using the pressure probe technique. Equation (30) for the calculation of the hydraulic conductivity of the plasmalemma is easily understood if one bears in mind that the term $(\alpha_1 k_1 + \alpha_2 k_2)$ in q describes the initial slope of the relaxation curve $s_p = (dP/dt)_{(t=0)}$. It shows clearly that at $t = 0$ only the hydraulic conductivity of the plasmalemma is important.

By solving Eq. (31) for P_e, the expression $P_e = P_o + \Delta P \cdot \pi^*_{op}/(\varepsilon + \pi^*_{op})$ is obtained. This is the turgor pressure at equilibrium following a relaxation and is completely analogous to the result from the two-compartment model [11]. This is expected since P_e is an equilibrium parameter and should be independent of the internal compartmentation of the cell.

In principle, Eq. (31) can be used to determine the reflection coefficient of the plasmalemma σ_p. Combining Eqs. (6) and (31) we obtain:

$$\sigma_p = \frac{\varepsilon}{\pi^s_{2o}} \cdot \frac{P_e - P_o}{P_i - P_e} - \frac{\pi^i_{2o}}{\pi^s_{2o}}. \tag{34}$$

The application of Eq. (34) is limited because the osmotic pressures π^i_{2o} and π^s_{2o} are usually not known. Furthermore, the entire analysis presented thus far has assumed that σ_p is close to 1, and solute flows have not been considered. Nevertheless, Eq. (31) is extremely useful in the case of a perfectly semipermeable membrane, i.e. for $\sigma = 1$ and $\pi^s_{2o} = 0$:

$$z = \frac{\pi^i_{2o}}{\varepsilon}. \tag{35}$$

The use of this relation for z in Eqs. (32) and (33) is preferable to that of the original definition, since the volumetric elastic modulus ε of the cell wall and the osmotic pressure of the cell sap π^i_{2o} can often be determined more accurately than the term $P_e - P_o$, which is small in the case of cells with large ε values.

Equation (32) yields the cytoplasmic volume V_2, if the total volume of the cell V_o was determined, either by measuring the dimensions of the cell under the microscope or by using the pressure-clamp technique [16]. The volume of the vacuole is then obtained using the relation $V_3 = V_o - V_2$.

The calculation of Lp_t from Eq. (33) requires an estimate for the surface area A_t as well as for the reflection coefficient σ_t of the tonoplast. Since the accuracy of such estimates is difficult to evaluate, statements about the hydraulic conductivity of the tonoplast may be subject to systematic errors. Even in the case of an ideally semipermeable membrane ($\sigma_t = 1$), without further assumptions about the surface area of the tonoplast, only the product $A_t \cdot Lp_t$ can be determined. If, for example, compartment 3 is divided into several vacuoles or if the tonoplast membrane is folded, Lp_t will be overestimated because the surface area is actually larger than was estimated by the cell's geometry. The possible condition $\sigma_t < 1$, on the other hand, leads to an underestimation of Lp_t.

An additional complication arises from the fact that the tonoplast can be permeable to solutes without affecting the stability of cell turgor pressure. Turgor pressure is influenced by solute flow and water flow through the plasmalemma. Since turgor pressure is the only parameter under observation, no information is gained about the solute permeability of the tonoplast from pressure relaxations. In the next section the extent to which this might affect the reliability of the calculated values for Lp_t is discussed.

Numerical Solution of the Flow Equations

In the preceding chapter, an analytical solution of the volume flow equations for the plasmalemma and the tonoplast was presented. The solute flow across both membranes had to be neglected for the sake of simplicity. It is a challenging question, however, to determine the extent to which the time course of a pressure relaxation is influenced by solute flow.

Let us first consider the plasmalemma alone. Here, a few simple observations lead to a qualitative understanding of the turgor pressure behavior in the presence of solute flow through the membrane. Consider what happens when a turgor pressure relaxation is initiated by adding a solute to which the plasmalemma is permeable. In this case, turgor pressure would pass a transient state due to the difference in transport rates of water and solute, but the eventual equilibration of solute concentration on both sides of the membrane would reset the osmotic gradient and the cell turgor pressure to the initial values present before the solute was added. Two phases of the pressure transient can readily be distinguished. An initial phase where water transport is predominant and a second phase where solute movement is predominant, but in the opposite direction. Recently, these phenomena were carefully examined by Steudle and Tyerman [9], who calculated values for the reflection coefficients and membrane permeabilities of several solutes from the biphasic turgor transient. In another case of interest, the plasmalemma is permeable to all solutes inside and outside the cell. As the concentrations would slowly equilibrate in both compartments, turgor would drop to zero. Both phenomena are easily detected experimentally. In experiments designed to measure Lp, turgor pressure is constant before and after the measurement. From this, we can conclude that net solute flow at the plasmalemma can generally be neglected. This is not necessarily true for the tonoplast. At equilibrium, there can be no hydrostatic pressure gradient or osmotic pressure gradient across the tonoplast. During exosmotic and endosmotic water flows, however, an osmotic gradient can develop across the tonoplast. Therefore, the solute permeability of the vacuolar membrane can influence the osmotic driving force for water flow between the cytoplasm and the vacuole. Thus, the time course of a pressure relaxation is not easily estimated.

When the plasmalemma is regarded as a perfectly semipermeable membrane and the tonoplast as a permeable membrane, we have the following set of phenomenological equations for the volume flows and the solute flows at the membranes:

Plasmalemma

$$J_{vp} = Lp_p\{P - (\pi^s_2 - \pi^s_1)\} \tag{36}$$

Tonoplast

$$J_{vt} = -Lp_t \cdot \sigma_t(\pi^s_3 - \pi^s_2) \tag{37}$$

$$J_{st} = (1 - \sigma_t)\bar{c}_s \cdot J_{vt} + \omega_t(\pi^s_3 - \pi^s_2) \tag{38}$$

where J_{st} = solute flow at the tonoplast, $\bar{c}_s$ = mean concentration of permeable solute, ω_t = coefficient of solute permeability P_s for the tonoplast, $\omega_t = P_s/(R \cdot T)$ and other parameters are as before (R and T have the usual meaning).

These equations were numerically integrated for various cell parameters using the computer program which is described in Appendix B. The results of this analysis are of special interest and will be considered in more detail.

Equation (38) tells us that J_{st} is the sum of a solvent drag term J'_s and a diffusion term J''_s given by

$$J'_s = (1 - \sigma_t)\bar{c}_s \cdot J_{vt} \tag{39}$$

and

$$J''_s = \omega_t(\pi^i_3 - \pi^s_2) \tag{40}$$

with

$$J_{st} = J'_s + J''_s. \tag{41}$$

As σ_t is less than or equal to unity and $\bar{c}_s$ is positive, the solvent drag J'_s has the same direction as the volume flow J_{vt}. If volume flow occurs from the vacuole to the cytoplasm, J_{vt} is positive by convention and J'_s is positive from Eq. (39). A positive volume flow at the tonoplast means that π^s_2 is larger than π^s_3 from Eq. (37). Consequently, J''_s is negative in this case from Eq. (40). Therefore, the two components of the solute flow have opposite directions. Figure 2 illustrates the situation at the two membranes during a pressure relaxation.

The following procedure will be applied to illustrate both the influence of the solvent drag J'_s and the diffusion flow J''_s at the tonoplast on the time course of a pressure relaxation, and the combined action of the two effects:

a) We take a computer program (Appendix B) which is able to account for side effects that were neglected in the analytical solution for pressure relaxations for the sake of simplicity.
b) We calculate a pressure relaxation with this computer program. The result should match reality better than the analytical solution.
c) We treat the result as if it were an experimental curve obtained in a real experiment.
d) We calculate the hydraulic conductivities by applying the calculus derived analytically to this hypothetical experiment.
e) We compare the result for Lp_p and Lp_t thus obtained with the value actually used in the computer program to create the curve.
f) We attribute the difference of the Lp_p- and Lp_t-values to the side effects that the computer program was able to account for, but that the analytical solution had to neglect.

The cell parameters chosen as input to the computer program (step a) were those obtained from a real pressure relaxation experiment with *Chara corallina*. The experiment is shown in Fig. 3 and was analyzed using the three-compartment model. (The simulation of a pressure relaxation on the basis of a related experiment makes a later comparison easier.) The cell parameters used were:

$V_o = 24.2\ \mu l$, $A_p = 121\ mm^2$, $A_t = 109\ mm^2$, $\varepsilon = 145$ bar,
$Lp_p = 4.3 \times 10^{-5}$ cm sec^{-1} bar^{-1}, $Lp_t = 3.1 \times 10^{-5}$ cm sec^{-1} bar^{-1},
$V_2/V_o = 7.2\%$, $\pi^s_2(t < 0) = \pi^s_3(t < 0) = 4.19$ bar,
$\pi^s_1 = 3.98$ bar (i.e. $\Delta P(t < 0) = 0.21$ bar), $\Delta P(t = 0) = 0.382$ bar.

Figure 4 shows the semilogarithmic plot of five numerically calculated pressure relaxation curves based on these data (step b). The plasmalemma was assumed to be perfectly semipermeable ($\sigma_p = 1$ and $\omega_p = 0$). The solute permeability P_s and the reflection coefficient σ_t of the tonoplast, however, varied for each curve as listed in Table 1. Note that $\sigma_t \cdot Lp_t$ was kept constant. Thus, differences in the driving force for volume flow at the tonoplast can clearly be

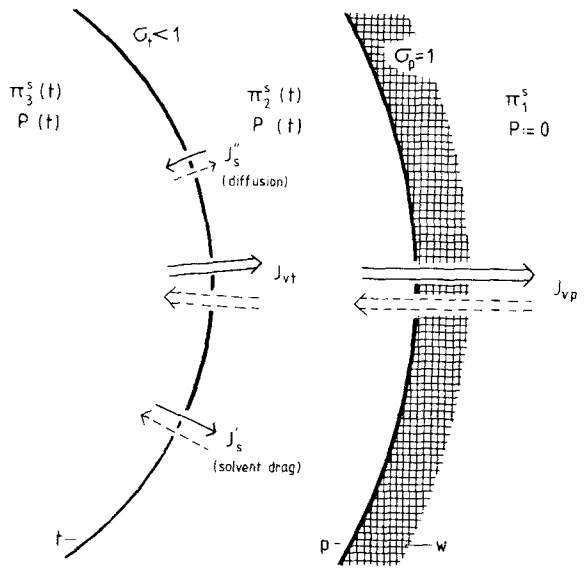

Fig. 2. Volume flows and solute flows at the plasmalemma and the tonoplast during a pressure relaxation. The pressure relaxation is supposed to be induced by a positive or negative pressure step ΔP. Volume flows are denoted by $\Rightarrow$ for $\Delta P > 0$ and by $\Leftarrow$ for $\Delta P < 0$, and solute flows by $\rightleftarrows$ for $\Delta P > 0$ and by $\leftrightarrows$ for $\Delta P < 0$. The tonoplast, which is subject to osmotic pressure differences alone, is assumed to be permeable. The plasmalemma is assumed to be impermeable to solutes. t = tonoplast, p = plasmalemma, w = cell wall, J_v = volume flow, J'_s = solvent drag, J''_s = diffusional flow, $P(t)$ = turgor pressure, π^i_k = osmotic pressure in compartment k (= 1, 2, 3)

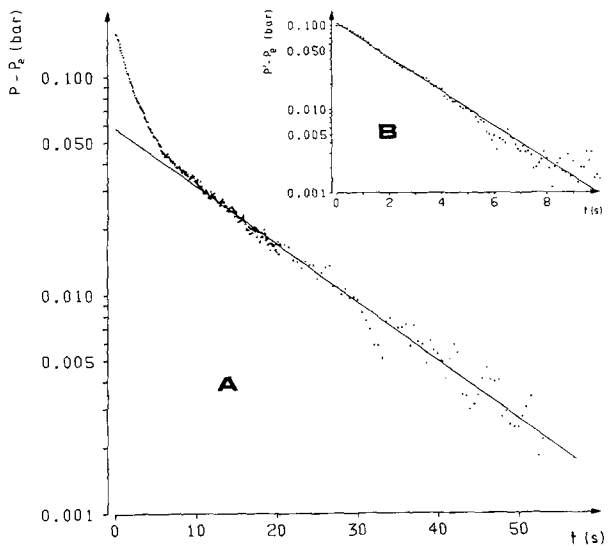

Fig. 3. Semilogarithmic plot of turgor relaxation in *Chara corallina*. A cell turgor of $P_o = 0.21$ bar was achieved by addition of sorbitol to the external medium (artificial pond water, for composition *see* following paper II). Two phases are clearly distinguishable (*A*). After subtraction of the slow component with an amplitude of 58 mbar and a half-time of 11.3 sec, an exponential function with an amplitude of 106 mbar and a half-time of 1.5 sec is obtained for the remaining values (*B*). An evaluation on the basis of the three-compartment model provides 4.3×10^{-5} cm sec^{-1} bar^{-5} of the hydraulic conductivity of the plasmalemma and 3.1×10^{-1} cm sec^{-1} bar^{-1} for that of the tonoplast. The cytoplasm was found to occupy 7.2% of the total volume. Cell data: $V_o = 24\ \mu l$, $A_p = 121\ mm^2$, $\varepsilon = 145$ bar. Assumptions: $\sigma_p = \sigma_t = 1.0$, $A_t = 109\ mm^2 = 0.9 \cdot A_p$

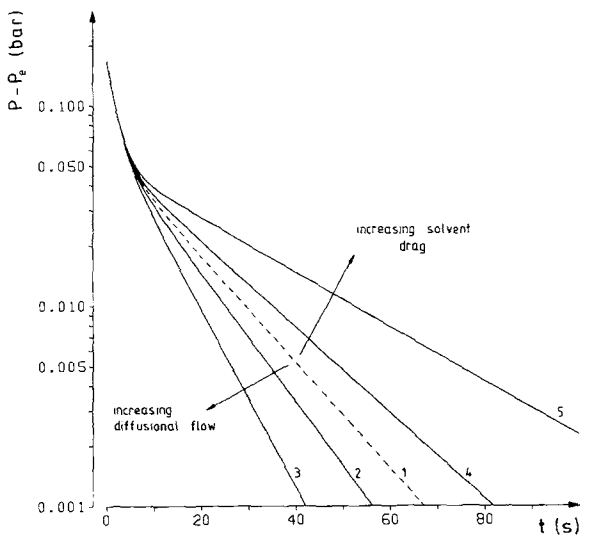

Fig. 4. Effect of diffusional flow and solvent drag across the tonoplast on numerically calculated turgor relaxations. The semilogarithmic plot demonstrates the effect of solute flow through the tonoplast. The plasmalemma was assumed to be impermeable to solutes. Curve 1 (dashed); without solute flow across the tonoplast. Curves 2 and 3: effect of a diffusional flow across the tonoplast. Curves 4 and 5: effect of solvent drag across the tonoplast. For the calculations, the cell parameters of Fig. 3 and the membrane parameters of Table 1 have been used

attributed to changes in the osmotic gradient (*see* Eq. 38).

Curve 1 (dashed) in Fig. 4 represents the course of the pressure relaxation for the ideal case $J_s = 0$ and corresponds to the measured curve illustrated in Fig. 3. In curves 2 and 3, only the diffusional flow at the tonoplast is considered while the solvent drag term vanished due to $\sigma_t = 1$. Diffusional flow had the effect of decreasing the half-time of the slow relaxation component and therefore speeding up the whole relaxation process. In curves 4 and 5, the solvent drag term was considered while diffusional flow was excluded because $P_s = 0$. This resulted in a decrease of the rate of the relaxation process, as the half-time of the slow relaxation component was increased. A more detailed explanation of these effects is given below.

Suppose now that the calculated curves of Fig. 4 were obtained as experimental curves from five different cells (step c). A reasonable concept would be to apply the mathematical calculus of the three-compartment model which was derived in the preceding chapter to the curves assuming that there are no solute flows either across the plasmalemma or across the tonoplast. First, the half-times and amplitudes of the two exponential compartments are determined by fitting the slow component of each curve to an exponential, subtracting this curve from the data set and fitting the remaining data to a second exponential function. The procedure can be done by hand or by computer as described in paper II. Then, Eqs. (30), (32), (33) and (35) are applied (step d). It should be kept in mind that these equations were derived for the special case of ideally semipermeable membranes.

Table 2 is a listing of the hydraulic conductivities of the plasmalemma and the tonoplast and the relative cytoplasmic volumes obtained from such an analysis. These values are now compared to those in brackets that have actually been chosen for the creation of the curves and are therefore referred to as the "true" values (step e). The agreement between the calculated and "true" values from the hydraulic conductivity of the plasmalemma Lp_p is fairly good for all curves. This agreement is also found in the case of the relative cytoplasmic volume.

However, deviations from the bracketed values occur for the hydraulic conductivity of the tonoplast Lp_t. In the case of curve 3, representing a strong solvent drag effect, Lp_t would have been

Table 1. Membrane parameters for the tonoplast used in numerically calculated pressure relaxations to demonstrate the effect of solvent drag and diffusional flow[a]

	$P_s = \omega_t \cdot R \cdot T$ (cm sec^{-1})	σ_t	Lp_t (cm sec^{-1} bar^{-1})
Curve 1:	0	1.0	3.1×10^{-5}
Curve 2:	3×10^{-5}	1.0	3.1×10^{-5}
Curve 3:	1×10^{-4}	1.0	3.1×10^{-5}
Curve 4:	0	0.8	3.9×10^{-5}
Curve 5:	0	0.5	6.2×10^{-5}

[a] The numbered curves refer to the curves shown in Figs. 4 to 6.

Table 2. Hydraulic conductivities of tonoplast and plasmalemma as derived from the theoretical pressure curves of Fig. 4[a]

	$Lp_p \cdot 10^5$ (cm sec^{-1} bar^{-1})	$Lp_t \cdot 10^5$ (cm sec^{-1} bar^{-1})	Relative cytoplasmic volume (%)
Curve 1:	4.4 (4.3)	3.1 (3.1)	7.1 (7.2)
Curve 2:	4.4 (4.3)	3.8 (3.1)	7.0 (7.2)
Curve 3:	4.5 (4.3)	5.4 (3.1)	6.9 (7.2)
Curve 4:	4.4 (4.3)	2.5 (3.9)	7.1 (7.2)
Curve 5:	4.3 (4.3)	1.5 (6.2)	7.1 (7.2)

[a] The values were calculated from the amplitudes and half-times of the two components of the relaxation processes using the key equations of the three-compartment model (Eqs. 30, 32, 33, 35). The values that were actually used for the construction of the curves are given in brackets. The discrepancy is due to a solute flow across the tonoplast which is neglected by the three-compartment model in its idealized form.

overestimated by 74%, whereas in the case of curve 5 representing a strong diffusion flow effect, Lp_t would have been underestimated by 76%. This finding clearly demonstrates that measurement of the hydraulic conductivity of the tonoplast is subject to a systematic error, due to the uncertainty about the solute flows occurring at the tonoplast (step f). In addition, there may be an error resulting from the uncertainty about the actual surface area of the tonoplast, as already discussed in the preceding chapter.

Now we turn to the question why pressure relaxations are retarded by solvent drag effects and accelerated by diffusional flow effects at the tonoplast. We must understand how the osmotic pressures in the cell compartments are influenced by solute flow at the vacuolar membrane, because they are part of the driving force for volume flow. Since the computer keeps track of the pressure behavior and that of the osmotic pressures and the compartment volumes during the iterations, π_2^s and π_3^s are readily obtained as functions of time.

Figure 5 shows the computer output for the osmotic pressures in the individual compartments, where each numbered curve corresponds to a pressure curve in Fig. 4 with the same numeral. The qualitative behavior of π_2^s and π_3^s will be explained with our attention focussed on curve 1. This curve represents the case of an ideally semipermeable tonoplast. The water flow across the plasmalemma at the onset of relaxation causes the osmotic pressure of the cytoplasm to increase rapidly (Fig. 5*A*, curve 1). The resulting osmotic gradient across the tonoplast then drives water out of the vacuole into the cytoplasm (Fig. 5*B*, curve 1). Curve 1 of Fig. 4 implies that turgor pressure drops rapidly at the same time, thus decreasing the driving force for water flow across the plasmalemma. At this moment, the volume flow from the vacuole to the cytoplasm predominates and the osmotic pressure of the cytoplasm decreases from its maximum (Fig. 5*A*, curve 1). After about 100 sec from the onset of the relaxation, π_2^s, π_3^s and $(P + \pi_1^s)$ have assumed the same value, and a new equilibrium is established.

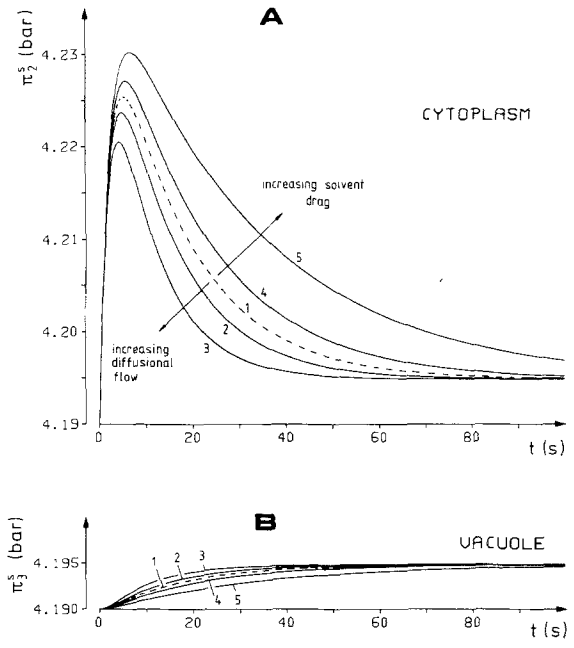

Fig. 5. Effect of diffusional flow and solvent drag across the tonoplast on the changes of the osmotic pressures in the cytoplasm (*A*) and the vacuole (*B*) during the calculated pressure relaxations shown in Fig. 4. Curve 1 (dashed): without solute flow across the tonoplast. Changes in π_2^s and π_3^s are due to the water flow across the plasmalemma and the tonoplast. Curves 2 and 3: effect of a diffusional flow across the tonoplast. Curves 4 and 5: effect of a solvent drag across the tonoplast. Solute permeabilities and reflection coefficients of the tonoplast for each curve are listed in Table 1

Diffusional flow through the tonoplast has the following effect. The greater the permeability of the

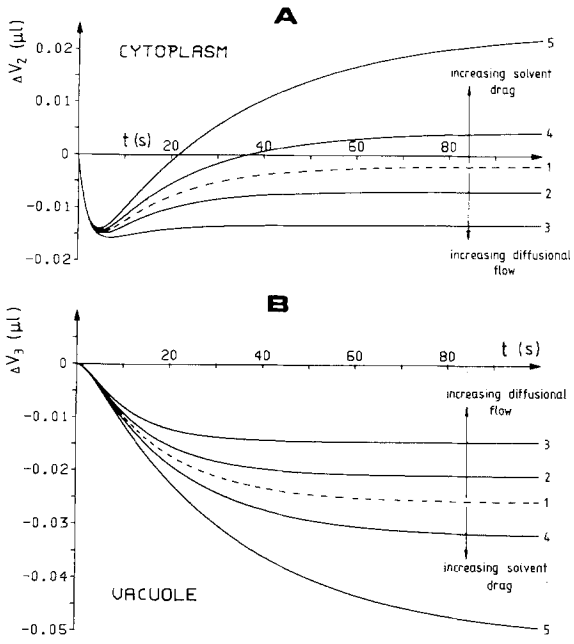

Fig. 6. Effect of diffusional flow and solvent drag across the tonoplast on volume changes of the cytoplasm (*A*) and the vacuole (*B*) during the pressure relaxations shown in Fig. 4. Curve 1 (dashed): without solute flow across the tonoplast. Curves 2 and 3: effect of a diffusional flow across the tonoplast. Curves 4 and 5: effect of a solvent drag across the tonoplast. Solute permeabilities and reflection coefficients of the tonoplast for each curve are listed in Table 1

tonoplast (Figs. 4 and 5, curves 2 and 3) the more particles follow the transient osmotic gradient from the cytoplasm into the vacuole ($\pi_3^s - \pi_2^s < 0$). This lessens the increase in the osmotic pressure of the cytoplasm and simultaneously maintains a greater driving force $P - (\pi_2^s - \pi_1^s)$ for water flow across the plasmalemma. Therefore, the volume loss from the cytoplasm is accelerated, and the half-time of the slow component is shortened (*cf.* Fig. 4, curves 2 and 3). Consequently, the cell that is represented by the three-compartment system reaches a new stationary state earlier than in the case where no solute flow is present.

When solvent drag instead of diffusion flow at the tonoplast is considered, the direction of solute movement is seen to reverse. As solute flow is coupled to water flow from the vacuole to the cytoplasm, the osmotic pressure of the cytoplasm is increased more (Fig. 5*A*, curves 4 and 5) relative to the case without solute flow (curve 1) and remains at a higher level for a longer time. At the same time, the driving force for volume flow across the plasmalemma is always smaller than before. This explains why the corresponding pressure relaxations (Fig. 4, curves 4 and 5) are slowed down.

Finally, Fig. 6 illustates how the volumes of the cell compartments change during the same hypothetical experiments. From the different plateau values reached at $t = 100$ sec it is understood that the total volume change of the cytoplasm and the vacuole is different depending on the case under consideration. For example, the vacuole loses more water when flow coupling occurs at the tonoplast than with an ideally semipermeable membrane (Fig. 6, curves 4 and 5, compared to curve 1). At the same time, the cytoplasm gains the corresponding amount. The reverse is true in the case of diffusional flow (Fig. 6, curves 2 and 3).

In reality, solute flows by diffusion and solvent drag always occur together, because both processes are dependent on the permeability of the membrane and therefore cannot be separated. Since the flows occur in opposite directions, the effects of the individual processes may cancel each other to some extent, depending on their magnitude. A permeable tonoplast may even behave like an ideally semipermeable membrane during pressure relaxation, if the effects cancel completely. This is the case when the following relationship between the reflection coefficient σ_t, the coefficient of solute permeability ω_t and the hydraulic conductivity Lp_t holds:

$$\omega_t = Lp_t \cdot \bar{c}_s(1 - \sigma_t)\sigma_t \tag{42}$$

where the mean concentration $\bar{c}_s = \frac{1}{2RT}(\pi_2^s(t) + \pi_3^s(t))$ is regarded as virtually constant. The changes of $\bar{c}_s$ in time are generally of the order of only 1% (Fig. 5), so that they can be neglected to a first approximation. To arrive at Eq. (42), we substituted J_{vt} in Eq. (38) by the right-hand side of Eq. (37), divided by $(\pi_3^s - \pi_2^s)$ ($\neq 0$ for $t \leq 0$) and solved ω_t for $J_{st} = 0$.

Conclusion

The compartmentation of a plant cell into vacuole and cytoplasm was considered with regard to its consequence for pressure relaxations. In the context of an extended view of a plant cell which we call the three-compartment model, the volume flow equations were solved analytically. It was assumed that the tonoplast and the plasmalemma were ideally semipermeable membranes. Under these assumptions, a pressure relaxation was shown to be the sum of *two* exponential functions. Theory shows that the magnitude of the hydraulic conductivities of the plasmalemma and the tonoplast can be evaluated from a single pressure relaxation if the resolution of the experiment is high enough to sepa-

rate the two exponential components. The reliability of values for the hydraulic conductivity of the tonoplast, however, depends on the knowledge of the surface area and the reflection coefficient of the tonoplast membrane. The evaluation of a pressure relaxation in the context of the three-compartment model also yields the volumes of the cytoplasm and the vacuole.

Allowing for solute flow across the tonoplast, the numerical solution of the flow equations showed that diffusional flow across the tonoplast alone had the effect of accelerating the pressure relaxation, whereas solvent drag alone resulted in a retardation of the pressure relaxation. In both cases, however, the two components of the relaxation curve could clearly be distinguished. As diffusional flow and solvent drag always occur together in a real plant cell, their effect on pressure relaxations may partially cancel each other. It is interesting to note that cases were shown to exist where a permeable tonoplast even behaves as if it were impermeable for solutes during a pressure relaxation.

We wish to thank Dr. K.-H. Büchner for numerous discussions. His stimulating interest in this work and his invaluable comments are gratefully acknowledged. Furthermore, we thank Drs. W.M. Arnold, K.-H. Büchner, G. Pilwat and E. Steudle for critical reading of the manuscript. This work was supported by a grant (SFB 160) from the Deutsche Forschungsgemeinschaft to U.Z.

References

1. Dainty, J. 1963. Water relations of plant cells. *Adv. Bot. Res.* **1**:279–326
2. Dainty, J. 1963. The polar permeability of plant cell membranes to water. *Protoplasma* **57**:220–228
3. Dainty, J. 1976. Water relations of plant cells. *In:* Encyclopedia of Plant Physiology, New Series. U. Lüttge and M.G. Pitman, editors. Vol. 2, pp. 12–35. Springer, Berlin—Heidelberg—New York
4. Dainty, J., Vinters, H., Tyree, M.T. 1974. A study of transcellular osmosis and the kinetics of swelling and shrinking in cells of *Chara corallina*. *In:* Membrane Transport in Plants. U. Zimmermann and J. Dainty, editors. pp. 59–63. Springer, Berlin—Heidelberg—New York
5. Kamiya, N., Tazawa, M. 1956. Studies on water permeability of a single plant cell by means of transcellular omosis. *Protoplasma* **46**:394–422
6. Kedem, O., Katchalsky, A. 1958. Thermodynamic analysis of the permeability of biological membranes to non-electrolytes. *Biochim. Biophys. Acta* **27**:229–246
7. Kiyosawa, K., Tazawa, M. 1977. Hydraulic conductivity of tonoplast-free *Chara* cells. *J. Membrane Biol.* **37**:157–166
8. Ritger, P.D., Rose, N.J. 1968. Differential Equations with Applications. McGraw-Hill, New York
9. Steudle, E., Tyerman, D.St. 1983. Determination of permeability coefficients, reflection coefficients, and hydraulic conductivity of *Chara corallina* using the pressure probe: Effects of solute concentrations. *J. Membrane Biol.* **75**:85–96
10. Steudle, E., Zimmermann, U. 1971. Hydraulische Leitfähigkeit von *Valonia utricularis*. *Z. Naturforsch.* **26b**:1302–1311
11. Steudle, E., Zimmermann, U. 1974. Determination of the hydraulic conductivity and of reflection coefficients in *Nitella flexilis* by means of direct cell-turgor pressure measurements. *Biochim. Biophys. Acta* **332**:399–412
12. Tazawa, M., Kamiya, N. 1965. Water relations of characean internodal cell. *Annu. Rep. Biol. Works, Fac. Sci. Osaka Univ.* **13**:123–157
13. Tyree, M.T. 1980. The water permeability of the tonoplast: Theoretical aspects. *In:* Plant Membrane Transport: Current Conceptual Issues. R.M. Spanswick, W.J. Lucas and J. Dainty, editors. pp. 459–460. Elsevier/North-Holland Biomedical, Amsterdam
14. Url, W.G. 1971. The site of penetration resistance to water in plant protoplasts. *Protoplasma* **72**:427–447
15. Walker, N.A., Pitman, M.G. 1976. Measurement of fluxes across membranes. *In:* Encyclopedia of Plant Physiology. U. Lüttge and M.G. Pitman, editors. New Series, Vol. 2, pp. 93–126. Springer, Berlin—Heidelberg—New York
16. Wendler, S., Zimmermann, U. 1982. A new method for the determination of hydraulic conductivity and cell volume of plant cells by pressure clamp. *Plant Physiol.* **69**:998–1003
17. Woolley, J.T. 1965. Radial exchange of labelled water in intact maize roots. *Plant Physiol.* **40**:711–717
18. Zimmermann, U. 1977. Cell turgor regulation and pressure mediated transport processes. *In:* Integration of Activity in the Higher Plant. D. Jennings, editor. pp. 117–154. Cambridge University Press, Cambridge
19. Zimmermann, U. 1978. Physics of turgor- and osmoregulation. *Annu. Rev. Plant Physiol.* **29**:121–148
20. Zimmermann, U. 1980. Pressure mediated osmoregulatory processes and pressure sensing mechanism. *In:* Animals and Environmental Fitness. R. Gilles, editor. pp. 441–459. Pergamon, Oxford
21. Zimmermann, U., Steudle, E. 1978. Physical aspects of water relations of plant cells. *Adv. Bot. Res.* **6**:45–117
22. Zimmermann, U., Steudle, E. 1980. Fundamental water relations parameters. *In:* Plant Membrane Transport: Current Conceptual Issues. R.E. Spanswick, W.J. Lucas and J. Dainty, editors. pp. 113–128. Elsevier/North-Holland Biomedical, Amsterdam

Received 7 August 1984; revised 2 January 1985

Appendix A

The first-order differential Eqs. (17) and (18) given in the text are transformed into a single second-order differential equation as follows:

$$\dot{P} + a \cdot P + b \cdot \Delta V_3 = c; \qquad \dot{P} := dP/dt \tag{17}$$

$$\Delta\dot{V}_3 + d \cdot \Delta V_3 + e \cdot P = f; \qquad \Delta\dot{V}_3 := d\Delta V_3/dt. \tag{18}$$

P and ΔV_3 are functions of time, the parameters a to f are constants. Solving Eq. (17) for ΔV_3 and Eq. (18) for $\Delta \dot{V}_3$ yields:

$$\Delta V_3 = \frac{1}{b}(c - \dot{P} - a \cdot P) \tag{A1}$$

$$\Delta \dot{V}_3 = f - d \cdot \Delta V_3 - e \cdot P. \tag{A2}$$

Combining Eqs. (A1) and (A2) yields:

$$\Delta \dot{V}_3 = f - \frac{d}{b}(c - \dot{P} - a \cdot P) - e \cdot P. \tag{A3}$$

The time-derivative of Eq. (17) is given by:

$$\ddot{P} + a \cdot \dot{P} + b \cdot \Delta \dot{V}_3 = 0; \qquad \ddot{P} := d^2P/dt^2. \tag{A4}$$

Combining and rearranging Eqs. (A3) and (A4) results in Eq. (20) of the text:

$$\ddot{P} + (a + d) \cdot \dot{P} + (a \cdot d - b \cdot e) \cdot P + (b \cdot f - d \cdot c) = 0. \tag{20}$$

Appendix B

For various applications, a computer program was used to integrate the set of phenomenological equations for volume flows and solute flows across the tonoplast and plasmalemma. The four coupled first-order differential equations given below were assumed to be valid.

Plasmalemma:

$$J_{vp} = Lp_p\{P - \sigma_p(\pi_2^s - \pi_1^s) - (\pi_2^i - \pi_1^i)\} \tag{B1}$$

$$J_{sp} = (1 - \sigma_p)\bar{c}_s \cdot J_{vp} + \omega_p(\pi_2^s - \pi_1^s) - J_a. \tag{B2}$$

Tonoplast:

$$J_{vt} = -Lp_t\{\sigma_t(\pi_3^s - \pi_2^s) + (\pi_3^i - \pi_2^i)\} \tag{B3}$$

$$J_{st} = (1 - \sigma_t)\bar{c}_s' \cdot J_{vt} + \omega_t(\pi_3^s - \pi_2^s) \tag{B4}$$

where J_{vp}, J_{vt} = volume flow at the plasmalemma/the tonoplast; J_{sp}, J_{st} = solute flow at the plasmalemma and the tonoplast; J_a = active solute uptake; P = turgor pressure; π_1^i, π_2^i, π_3^i = osmotic pressure of the impermeable solutes in the external space/the cytoplasm/the vacuole; π_1^s, π_2^s, π_3^s = osmotic pressure of the permeable solute in the external space/the cytoplasm/the vacuole; Lp_p, Lp_t = hydraulic conductivity of the plasmalemma/the tonoplast; σ_p, σ_t = reflection coefficient of the plasmalemma/the tonoplast; ω_p, ω_t = coefficient of the solute permeability for the plasmalemma/the tonoplast ($\omega = P_s/(R \cdot T)$); $\bar{c}_s$, $\bar{c}_s'$ = mean concentration of the permeable solute on both sides of a membrane, different for plasmalemma and tonoplast.

A simple iteration technique, known as Euler's method [8], was used to integrate the differential equations above. FORTRAN was used as the programming language, and calculations were carried out using 'double precision' variables (16-digit accuracy). The time increment $\Delta t = 0.1$ sec was usually sufficient. The calculations were carried out with the aid of a MINC-11 computer (Digital Equipment Corporation, Cologne, W. Germany). The results were temporarily stored on a floppy disk and graphically displayed by a programmable plotter (Plotter 281, GDV Tübingen, W. Germany).

The flexibility of the program allowed the system of flow equations to be solved for one or two membranes in series (i.e. in the context of the two-compartment model or three-compartment model). Furthermore, either a constant volumetric elastic modulus ε or a linear dependence of ε on turgor pressure could be accounted for. There was also an option of including or omitting solute flows across the membranes. A constant solute uptake at the plasmalemma could be simulated by including a constant J_a in Eq. (B2). By variation of membrane parameters, further degrees of freedom were obtained. With $\omega = 0$ and $\sigma_t < 1$, the effect of solvent drag at the tonoplast was investigated in isolation from the effect of diffusional flow which was examined by choosing $\omega \neq 0$ and $\sigma_t = 1$.

Although the program provided for a more realistic simulation of pressure relaxations than the analytical solution did, a few simplifications were made here as well. Thus, the volume changes in the compartments due to the small amount of solute being transferred were neglected. Furthermore, the activity coefficients of the solutes were assumed to be 1 in order to simplify the relation between the solute concentrations and the osmotic pressures in the compartments.